Available online at www.sciencedirect.com
ScienceDirect
Ceramics International 37 (2011) 819–824
CERAMICS INTERNATIONAL
www.elsevier.com/locate/ceramint

Sodium impurities in $ZnO–Bi_2O_3–Sb_2O_3$ based varistors

M. Peiteado *, Y. Iglesias, A.C. Caballero

Department of Electroceramics, Instituto de Cerámica y Vidrio, CSIC, Kelsen 5, 28049 Madrid, Spain

Received 16 July 2010; received in revised form 10 August 2010; accepted 10 October 2010
Available online 17 November 2010

Abstract

Sodium impurities are frequently present in the raw oxides that constitute the complex formulation of $ZnO–Bi_2O_3–Sb_2O_3$ based varistors. But actually little is known about their effect on the microstructure and the electrical response of these materials. This is the main goal of the present contribution and according to the obtained results an excessive presence of this alkaline impurity can lead to a compositional change in the Bi-rich skeleton of the varistor microstructure. As a consequence the grain growth kinetics, the densification rate and the characteristic non-linear I–V response of these electroceramics are seriously affected.

Keywords: A. Grain growth; C. Electrical conductivity; D. ZnO; E. Varistors; Alkaline impurities

1. Introduction

The formulation of ZnO-based varistors entails a complex multicomponent system around which still exits a qualitative knowledge more than quantitative accurate information of the role played by each component [1]. The configuration of stable potential barriers along the entire microstructure of these non-linear ceramics requires a uniform distribution of the dopants [2–6]. Consequently a high degree of homogeneity in the starting ceramic powder should be, actually is, a compulsory condition. But in the same way the presence of impurities, either incorporated during the processing steps or included in the starting raw materials, has to be carefully controlled [7,8]. For example alkaline impurities represent a major threat since they are frequently present in the raw oxides, including the minority dopants. However, although these alkaline ions are usually avoided, little is in fact known about their effect on the microstructure and electrical response of ZnO varistors. Most of the existing literature just links this type of impurities, especially sodium, with the varistor stability against degradation. For example, assuming that the migration of zinc interstitials to the depletion layer is the main mechanism leading to the degradation of the potential barrier, Gupta et al. developed a theoretical model in which the presence of a small amount of Na^+ ions in the interstitials positions (<280 ppm) could help to block such migration of zinc ions [9,10]. However there is no clear evidence of the sodium ions entering the ZnO grains or even the depletion layer at the grain boundaries. Later on, Kutty and Ezhilvalavan claimed that Na impurities could increase the density of trap states at the interfaces, and so enhance the non-linearity of the sintered ceramics [11]. This last work was run on simplified varistor compositions, so a different behaviour might be obtained in a complete varistor formulation. But the case is that none of these reports discussed the effect of sodium impurities on the microstructure development of these electroceramics. In varistors based on the $ZnO–Bi_2O_3$ classical system, the densification process, the grain growth kinetics and the distribution of the different dopants through the ceramic body, strongly depend on the particular characteristics of the Bi-rich liquid phase which forms during the sintering stage [12–14]. From the field of glass and glass–ceramics, sodium is known to play a determinant role as a flux agent, contributing as well to the decrease in the viscosity of the liquid phase [15]. In this sense, any involuntary excess of alkali impurities might exert a severe influence on the proper development of the varistor microstructure and, consequently, on its electrical properties.

Within this framework, in the present contribution we have intentionally incorporated different amounts of sodium to the

* Corresponding author. Tel.: +34 917355840; fax: +34 917355843.
E-mail address: mpeiteado@icv.csic.es (M. Peiteado).

0272-8842/$36.00
doi:10.1016/j.ceramint.2010.10.016

varistor formulation in order to more precisely describe the effect of such common impurities on the varistor microstructure and its electrical response.

2. Materials and methods

The role of sodium impurities was analyzed on four different compositions prepared from a commercial varistor powder based on the $ZnO–Bi_2O_3–Sb_2O_3$ (ZBS) system and with different contents of sodium: 0, 100, 1000 and 10,000 ppm of Na^+. In all cases sodium was incorporated to the formulation by mixing sodium bicarbonate ($NaHCO_3$ reagent grade from Fluka) with the varistor powder on a planetary mill for 2 h in ethanol. Dense materials were then obtained using a classical mixed-oxide route. The dried powders were sieved under 100 μm and uniaxially pressed at 120 MPa into pellets approximately 12 mm in diameter and thickness. Sintering of the green compacts was carried out at 1140, 1180 and 1220 °C, with a soaking time of 4 h. Also experiments were conducted at a fixed maximum temperature of 1180 °C with soaking times up to 24 h.

Phase characterization of the starting powders was performed by X-ray diffraction (XRD) in a D5000 Siemens Diffractometer using Cu $K_{\alpha 1}$ radiation. Densities of the sintered samples were measured using the water-immersion method. For microstructure observations scanning electron microscopy of polished and chemically etched (acetic acid, 10% diluted) surfaces was carried out using a cold field emission-scanning electron microscope (FE-SEM Model S-4700, Hitachi) equipped with an energy dispersive spectroscopy (EDS) microanalysis probe. ZnO grain size was evaluated from FE-SEM micrographs by an image processing and analysis program that measures the surface of each ZnO grain and transforms its irregularly shaped area into a circle of equivalent diameter. Statistical estimations were performed over more than 800 grains.

For electrical characterization, sintered samples were cut into discs 3 mm thick and Ag electroded. Standard *V–I* measurements were carried out using a dc power multimeter (Keithley 2410). The varistor breakdown field E_{eff} was estimated at a current density of 5 mA/cm^2. The density of leakage currents J_L was measured at a voltage corresponding to the 85% of the breakdown voltage. Finally the non-linear coefficient α was measured in the current density range between 5 and 20 mA/cm^2. For ac measurements an Agilent 4294A impedance analyzer was used in the range 40 Hz to 1 MHz. Measurements were taken at different temperatures by placing the sample on a home made electrical furnace.

3. Results and discussion

3.1. Microstructure characterization

XRD patterns shown in Fig. 1 correspond to the samples treated at 1140 °C/4 h. In all cases diffraction peaks corresponding to the major ZnO hexagonal phase are obtained (JCPDS card no 36-1451), together with some secondary peaks

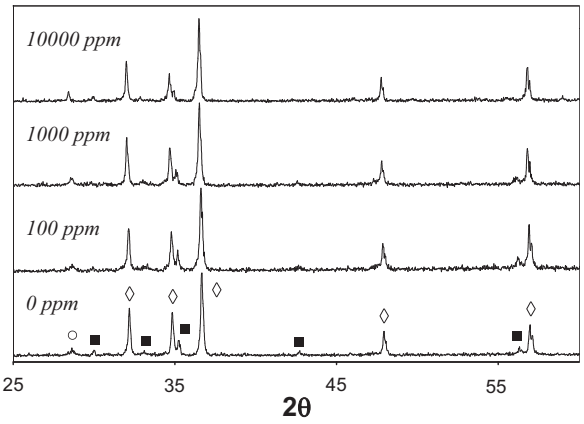

Fig. 1. XRD patterns of the compositions with different amounts of added sodium after sintering at 1140 °C/4 h. (◇) ZnO, (■) $Zn_7Sb_2O_{12}$ and (○) Bi_2O_3.

attributed to the $Zn_7Sb_2O_{12}$ spinel and the Bi_2O_3 phases (JCPDS cards no 15-0687 and no 41-1449, respectively). Actually this is the characteristic distribution of crystalline phases for a varistor formulation based in the ZBS ternary system [16,17], and indicates that even for the higher amount of added sodium (10,000 ppm) the formation of a new Na-containing secondary phase is not observed. Similar results were obtained when the compositions were sintered at 1180 and 1220 °C and, furthermore, for all the tested temperatures no substantial shift in the peaks positions was observed with the addition of sodium, so initially, a systematic incorporation of Na ions into the ZnO lattice cannot be presumed or at least it cannot be detected by XRD analyses.

The microstructure of the prepared ceramics was then examined on the microscope. Fig. 2 depicts the FE-SEM micrographs of the samples sintered at 1140 °C/4 h. Initially the four compositions again show the same overall microstructure, comprising big and regularly twinned ZnO grains, smaller grains of the spinel phase (mainly located at triple and multiple points) and a skeleton of different Bi-rich phases surrounding all these grains. As it is known the K_α lines of Na overlap in energy with the L_α lines of Zn (1041 and 1011.7 eV, respectively) so any attempt to identify the presence of sodium by EDS was futile. However, two distinguishable effects were observed as the amount of sodium is increased. First, as visibly illustrated in the images of Fig. 2 the samples become more sensible to the chemical etching as the amount of sodium is augmented. Second, a gradual increase in the average size of ZnO grains was also obtained with the addition of sodium. Data in Table 1 more clearly depicts the increase in the grain size (in some cases measurements were done from not chemically etched surfaces), but the fact is that both mentioned effects can actually be attributed to the same feature: the incorporation of sodium into the Bi-rich secondary phase. On one hand the chemical etching was run with acetic acid and acids strongly etch the Bi-rich phases [18]. Since as observed the efficiency of the etching increases with the increase in the amount of added sodium, it is likely that this impurity would preferentially incorporate into the Bi-

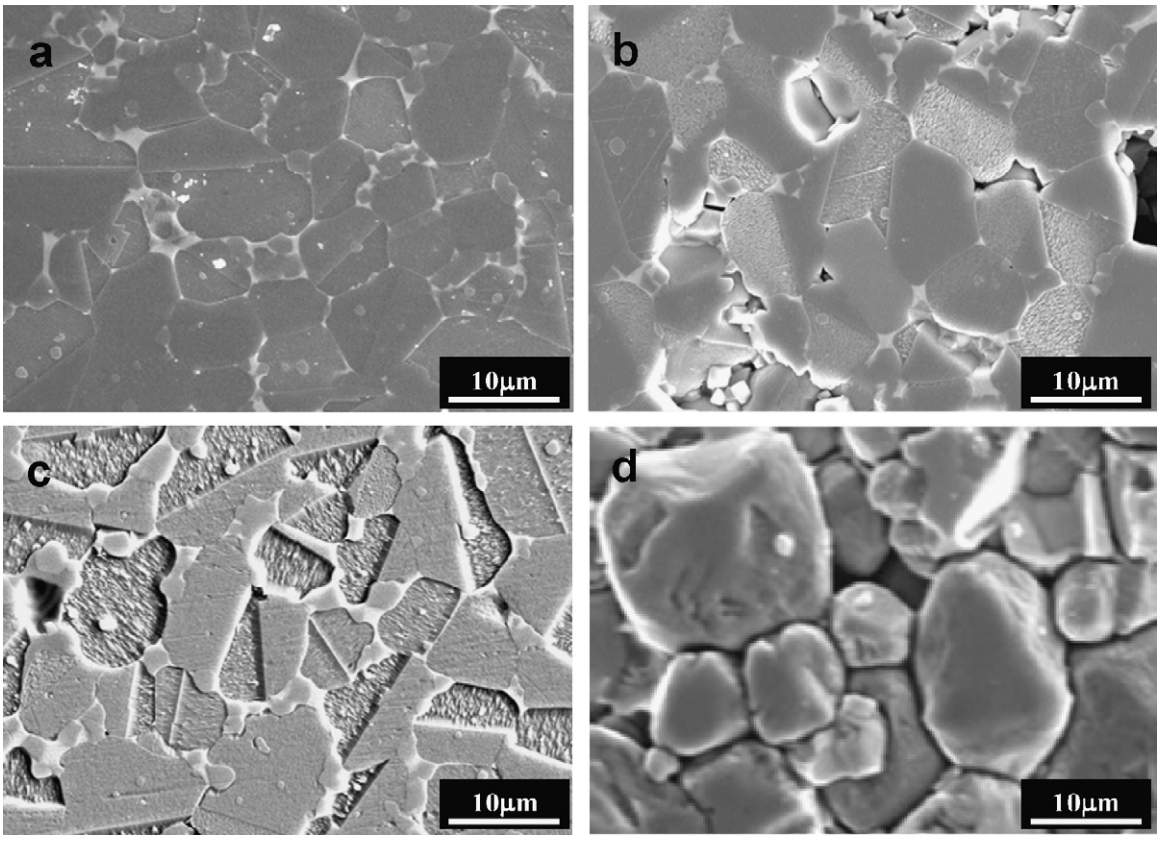

Fig. 2. FE-SEM images of polished and chemically etched surfaces of samples of compositions (a) 0Na, (b) 100Na, (c) 1000Na and (d) 10,000Na, after sintering at 1140 °C/4 h.

rich phases; in other words, the addition of sodium promotes a compositional change in the skeleton of bismuth which makes it more susceptible to the attack with acid. On the other hand the enhancement of the grain growth process is consistent with an increase in the kinetics of mass transport; in our ZBS system sintering takes place in the presence of a liquid phase, so an increase in the growth kinetics could be attributed to a decrease in the viscosity of the liquid. Since, as mentioned in Section 1, the higher the amount of sodium in the liquid the lower its viscosity [15], again we can presume that the observed change in ZnO grain size points towards the presence of sodium in the Bi-rich phase.

Increasing the sintering temperature initially leads to a similar microstructure that the one observed at 1140 °C. FE-SEM images of Fig. 3 correspond to the sample with 10,000 ppm of Na treated at 1180 °C/4 h and again evidence is observed of the higher sensibility of this composition to the chemical etching. A more detailed image of the Bi-rich phase that remained after the acetic attack is shown in Fig. 3c; the track of the acid can be inferred from the small hollow cavities in the bright whitish phase. No sodium was detected on the EDS analyses of this Zn-free area, but this time because it has been mostly removed by the acid attack. Regarding the ZnO grain size, it now increases because of both the effect of the higher temperature and the effect of sodium. In this sense Fig. 4 depicts the evolution of the ZnO grain size as a function of the sintering temperature and the amount of added sodium. As observed the differences become remarkable for the composition with 10,000 ppm of sodium, with average sizes doubling those of the sample without extra sodium. This particular composition however has its own drawback, characterized by a worrisome poor densification. Data in Table 2 depict the evolution of density as a function of the amount of sodium and it can be observed that independently of the sintering temperature, the lower density values are those of the composition with 10,000 ppm of Na^+. Moreover, these data

Table 1
Evolution of ZnO average grain size as a function of the amount of added sodium for the samples sintered at 1140 °C/4 h.

Sintering: 1140 °C/4 h	G_{ZnO} (±0.5 μm)
0Na (commercial varistor)	7.8
100Na (100 ppm Na^+)	8.5
1000Na (1000 ppm Na^+)	9.4
10,000 Na (10000 ppm Na^+)	15.0

Table 2
Evolution of density with the sintering temperature ($\rho \pm 0.1$ g/cm^3) for the different compositions tested in this study. Soaking time = 4 h.

	0Na	100Na	1000Na	10,000Na
1140 °C/4 h	5.4	5.4	5.3	5.1
1180 °C/4 h	5.3	5.3	5.2	5.0
1220 °C/4 h	5.3	5.3	5.2	5.0

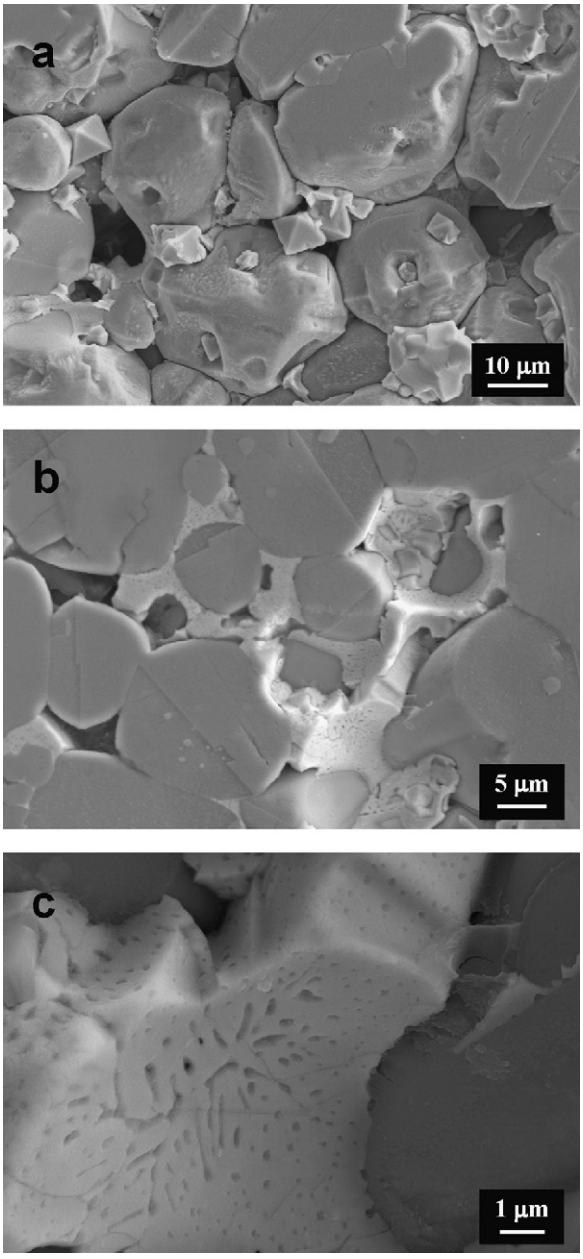

Fig. 3. FE-SEM images of sample with 10,000 ppm of sodium (10,000Na) after sintering at 1180 °C/4 h. The smaller octahedral-shaped particles in image (a) correspond to the secondary $Zn_7Sb_2O_{12}$ spinel phase. Images b and c show a detailed picture of the Bi-rich secondary phase (liquid during sintering) which remained after the chemical etching of the polished surface.

also show that the decrease in density starts to be noticeable for the sample with 1000 ppm of sodium. Once again the results should be interpreted in terms of the change on the nature of the Bi-rich liquid phase promoted by the increased incorporation of sodium. As a result of this change some occluded porosity can be formed that cannot be removed during the retracement of the liquid to the multiple points between ZnO grains [19], so higher values of density cannot be achieved. Furthermore, in our materials the problems with densification for the composition with 10,000 ppm of added Na^+ were such that finally it had to be discarded for further electrical characterization.

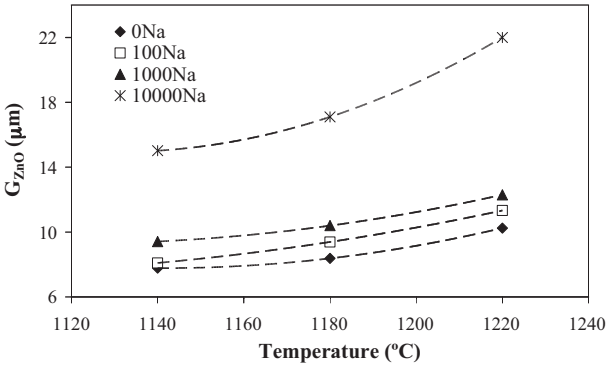

Fig. 4. Evolution of ZnO average grain size for the samples with different amounts of sodium as a function of sintering temperature (soaking time = 4 h).

To finish with the microstructure characterization, different sintering experiments were conducted varying the soaking time at the maximum temperature. Apart from the expected grain growth with the sintering time, the obtained results (not depicted here) again revealed a decrease in density and an increase in the grain size as more sodium is incorporated to the ceramic, to the Bi-rich liquid phase.

3.2. Electrical characterization

Fig. 5 shows the characteristic *J–E* curves for the samples with different amounts of added sodium and sintered at different sintering temperatures. As observed all compositions show a marked non-linear response, with an abrupt transition between the high and low resistivity regions. Coherently with the observed increase in the ZnO grain size, the varistor breakdown field decreases with the amount of added sodium as well as with the sintering temperature [20]. These data are better displayed in Table 3, together with the evolution of the non-linear coefficient α and the density of leakage currents. For all tested temperatures (and soaking times as well, not shown here) a general impoverishment of the varistor response is observed when sodium is incorporated to the formulation: the higher the amount of sodium, the lower the value of α and the higher the density of leakage currents. Furthermore, this

Table 3
Evolution of the varistor electrical parameters with temperature for the compositions with different amounts of added sodium (soaking time = 4 h). In all cases the measurement uncertainties were of 3% for the breakdown field E_{eff}, of 5% for the non-linear coefficient α and of 25% for the density of leakage currents J_L.

	E_{eff} (kV/cm)	J_L (mA/cm^2)		α
1140 °C	0 ppm Na^+	2852	0.008	47
	100 ppm Na^+	2437	0.112	35
	1000 ppm Na^+	2436	0.191	31
1180 °C	0 ppm Na^+	2474	0.006	52
	100 ppm Na^+	2287	0.128	39
	1000 ppm Na^+	1967	0.280	27
1220 °C	0 ppm Na^+	2176	0.006	54
	100 ppm Na^+	1800	0.231	37
	1000 ppm Na^+	1484	0.356	30

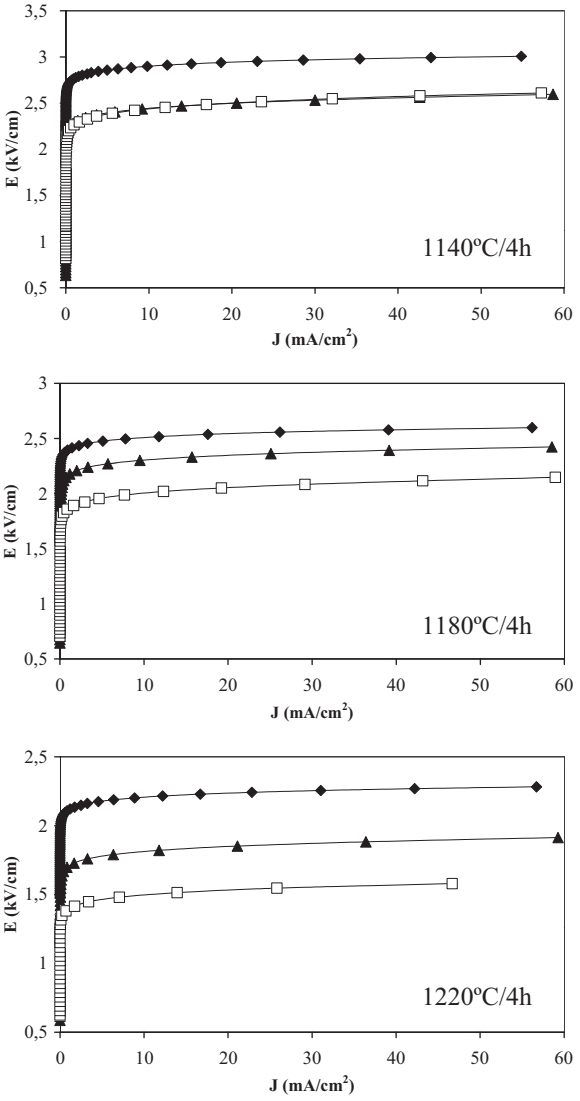

Fig. 5. Standard *J–E* curves of the samples with different amounts of added sodium as a function of sintering temperature (soaking time = 4 h). (◆) 0 ppm Na^+, (▲) 100 ppm Na^+, (□) 1000 ppm Na^+.

detrimental increase in the leakage currents, of approximately two orders of magnitude, is even more noticeable at higher temperatures as can be observed in Table 3.

The impoverishment of the electrical parameters with the addition of sodium can be explained by two main effects. On one hand and in agreement with the previous microstructure characterization, the change in the nature of the Bi-rich secondary phase is leading to a preferential conduction path along the varistor microstructure; i.e., the presence of sodium in the skeleton of bismuth contributes to increase its conductivity and this leads to an unacceptable increase of the leakage currents, the current through the varistor in the pre-breakdown region. Subsequently the non-linear response of the ceramic also decreases. But on the other hand the lower value of α might be as well attributed to a general decrease in the height of the potential barriers at grain boundaries. This would imply a straight involvement of sodium impurities in the configuration of the barriers, by incorporating into the depletion layer as suggested in the literature [10]. However this second possibility cannot be easily confirmed by just performing a detailed microstructure characterization, as can be inferred from the previous section. So at this point the analysis by impedance spectroscopy might be helpful. Actually, as a useful tool for detecting relevant changes on the conduction mechanisms, in the last years different analyses by impedance spectroscopy, in any of its possible formalisms, have been reported on ZnO-base materials [21–25]. The choice between formalisms depends not only on the material's electrical response but also on the set of parameters that are going to be analyzed. In our particular case, since the changes observed in the varistor microstructure mostly concern to the skeleton of Bi-rich phases, the analysis of the highly conducting ZnO grain cores is really not required. Hence, by applying the impedance formalism [23] and by taking measurements at relatively high temperatures (>150 °C), the resistivity of the material, mainly dominated by the Bi-rich secondary phase, can be obtained by fitting the response to a parallel RC circuit. Fig. 6 then shows the representative impedance plots for the different Na-containing compositions. As observed, while the electrical response of the sample with no extra sodium perfectly fits with a single RC circuit, the addition of Na^+ to the varistor formulation requires the incorporation of a constant phase element (CPE) to the equivalent circuit. Moreover, the inclusion of this CPE better describes the electrical response than the fit with two parallel RC circuits, as it was previously suggested [23]. This can be indicative of the existence of different regions with small variations in the capacitance values; i.e., the incorporation of sodium can lead to a certain compositional heterogeneity in the Bi skeleton that has its reflection in a heterogeneous electrical response. However in order to confirm if there are also changes in the dominant conduction mechanism, the total resistivity of the material has to be as well estimated. In this sense the Arrhenius plot of Fig. 7 is obtained from the value of the low frequency intercept of the impedance plots. As observed the conductivity slightly decreases with the amount of sodium, but

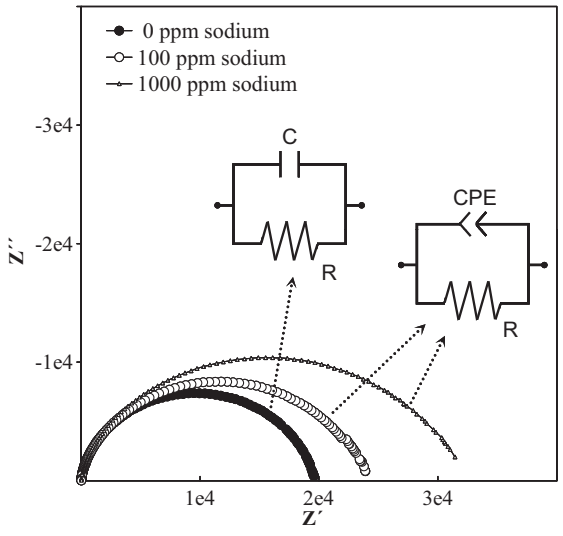

Fig. 6. Z'' vs. Z' Argand diagrams for the compositions sintered at 1180 °C/4 h. Temperature of measurement: 350 °C.

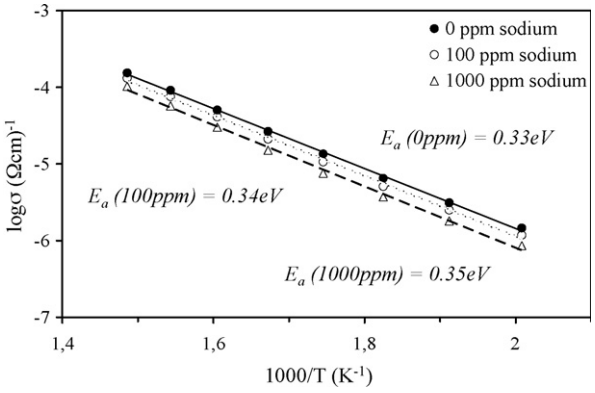

Fig. 7. Arrhenius plot of the electrical conductivity as calculated from the impedance measurements. Calculated activation energies are depicted in the plot.

the activation energy stays in similar values to that of the sample with no extra Na. In other words, although the dominant conduction mechanism remains unaltered some quantitative changes can be observed.

Therefore, the microstructure changes promoted by the incorporation of sodium certainly modify the electrical behaviour of the Bi-rich skeleton and, consequently, will also affect to the formation of the potential barriers. However this alteration is of quantitative nature and then it could be ascribed to two combined effects: the injection of charge carriers (conduction along boundaries) and the formation of a smaller fraction of good (active) potential barriers.

4. Conclusions

The pernicious effect of sodium impurities on the microstructure and the electrical response of ZBS-based varistors have been analyzed on samples prepared by conventional solid state route. The microstructure characterization of these samples evidences a compositional change in the skeleton of Bi phases. The incorporated sodium modifies the Bi-rich liquid phase and as a consequence the grain growth kinetics and the densification rate are significantly altered. With regards to the electrical response, a manifest decrease in the varistor non-linear coefficient together with an unacceptable increase of the leakage currents in stand-by conditions is observed with the increased presence of the alkaline impurity. Although the precise role of sodium ions in the formation of the potential barriers cannot be clarified (in terms of defects), the electrical characterization certainly shows that the conduction along the Bi-rich skeleton increases with the addition of sodium.

Acknowledgements

This work has been conducted within CICYT MAT 2007-65857 and CICYT MAT 2007-66845-C02-01 projects.

References

[1] D.R. Clarke, Varistor ceramics, J. Am. Ceram. Soc. 82 (1999) 485–502.
[2] Z. Brankovic, G. Brankovic, S. Bernik, M. Zunic, ZnO varistor with reduced amount of additives prepared by direct mixing of constituent phases, J. Eur. Ceram. Soc. 27 (2007) 1101–1104.
[3] M.A. Ramírez, A.Z. Simoes, M.A. Márquez, Y. Maniette, A.A. Cavalheiro, J.A. Varela, Characterization of ZnO-degraded varistors used in high-tension devices, Mater. Res. Bull. 42 (2007) 1159–1168.
[4] P.R. Bueno, J.A. Varela, E. Longo, SnO_2, ZnO and related polycrystalline compound semiconductors: an overview and review on the voltage-dependent resistance (non-ohmic) feature, J. Eur. Ceram. Soc. 28 (2008) 505–529.
[5] S. Bernik, G. Brankovic, S. Rustja, M. Zunic, M. Podlogar, Z. Brankovic, Microstructural and compositional aspects of ZnO-based varistor ceramics prepared by direct mixing of the constituent phases and high energy milling, Ceram. Int. 34 (2008) 1495–1502.
[6] M. Takada, S. Yoshikado, Effect of thermal annealing on electrical degradation characteristics of Sb–Bi–Mn–Co-added ZnO varistors, J. Eur. Ceram. Soc. 30 (2010) 531–538.
[7] Y. Yano, Y. Takai, H. Morooka, Interface states in ZnO varistor with Mn, Co, and Cu impurities, J. Mater. Res. 9 (1994) 112–118.
[8] J.W. Fan, R. Freer, The roles played by Ag and Al dopants in controlling the electrical-properties of ZnO varistors, J. Appl. Phys. 77 (1995) 4795–4800.
[9] T.K. Gupta, W.G. Carlson, A grain-boundary defect model for instability/stability of a ZnO varistor, J. Mater. Sci. 20 (1985) 3487–3500.
[10] T.K. Gupta, A.C. Miller, Improved stability of the ZnO varistor via donor and acceptor doping at the grain boundary, J. Mater. Sci. 3 (1988) 745–754.
[11] T.R.N. Kutty, S. Ezhilvalavan, Influence of alkali ions in enhancing the nonlinearity of ZnO–Bi_2O_3–Co_3O_4 varistor ceramics, Jpn. J. Appl. Phys. 34 (1995) 6125–6132.
[12] M.A. De la Rubia, M. Peiteado, J.F. Fernández, A.C. Caballero, Study at the Bi_2O_3-rich region of the ZnO–Bi_2O_3 system, Bol. Soc. Ceram. V. 43 (2004) 745–747.
[13] Y.W. Lao, S.T. Kuo, W.H. Tuan, Effect of Bi_2O_3 and Sb_2O_3 on the grain size distribution of ZnO, J. Electroceram. 19 (2007) 187–194.
[14] D. Xu, L.Y. Shi, Z.H. Wu, Q.D. Zhong, X.X. Wu, Microstructure and electrical properties of ZnO–Bi_2O_3-based varistor ceramics by different sintering processes, J. Eur. Ceram. Soc. 29 (2009) 1789–1794.
[15] J.M. Fernández Navarro, El Vidrio: Constitución, Fabricación Propiedades, third ed., Consejo Superior de Investigaciones Científicas, Madrid, 2003.
[16] E. Olsson, G. Dunlop, R. Österlund, Development of functional microstructure during sintering of a ZnO varistor material, J. Am. Ceram. Soc. 76 (1993) 65–71.
[17] M. Peiteado, M.A. De La Rubia, J.F. Fernández, A.C. Caballero, Thermal evolution of ZnO–Bi_2O_3–Sb_2O_3 system in the region of interest for varistors, J. Mater. Sci. 41 (2006) 2319–2325.
[18] W. Jo, S.J. Kim, D.Y. Kim, Analysis of the etching behavior of ZnO ceramics, Acta Mater. 53 (2005) 4185–4188.
[19] M.N. Rahaman, Ceramic Processing and Sintering, second ed., Marcel Dekker, New York, 2003.
[20] M. Peiteado, J.F. Fernandez, A.C. Caballero, Varistors based in the ZnO–Bi_2O_3 system: Microstructure control and properties, J. Eur. Ceram. Soc. 27 (2007) 3867–3872.
[21] M. Andres-Verges, A.R. West, Impedance and modulus spectroscopy of ZnO varistors, J. Electroceram. 1 (1997) 125–132.
[22] Y.W. Hong, J.H. Kim, Impedance and admittance spectroscopy of Mn_3O_4-doped ZnO incorporated with Sb_2O_3 and Bi_2O_3, Ceram. Int. 30 (2004) 1307–1311.
[23] D. Fernández-Hevia, M. Peiteado, J. de Frutos, A.C. Caballero, J.F. Fernández, Wide range dielectric spectroscopy of ZnO-based varistors as a function of sintering time, J. Eur. Ceram. Soc. 24 (2004) 1205–1208.
[24] P.R. Bueno, J.A. Varela, E. Longo, Admittance and dielectric spectroscopy of polycrystalline semiconductors, J. Eur. Ceram. Soc. 27 (2007) 4313–4320.
[25] M. Slankamenac, T. Ivetic, M.V. Nikolic, N. Ivetic, M. Zivanov, V.B. Pavlovic, Impedance response and dielectric relaxation in liquid-phase sintered Zn_2SnO_4–SnO_2 ceramics, J. Electron. Mater. 39 (2010) 447–455.